Space Sci Rev (2009) 143: 31–42
DOI 10.1007/s11214-008-9429-x

Influence of the Interstellar Magnetic Field and Neutrals on the Shape of the Outer Heliosphere

N.V. Pogorelov · J. Heerikhuisen · G.P. Zank · S.N. Borovikov

Received: 21 March 2008 / Accepted: 16 August 2008 / Published online: 17 September 2008

Abstract Formed as a result of the solar wind (SW) interaction with the circumheliospheric interstellar medium (CHISM), the outer heliosphere is generically three-dimensional because of the SW asphericity and the action of the interstellar and interplanetary magnetic fields (ISMF and IMF). In this paper we show that charge exchange between neutral and charged components of the SW–CHISM plasmas plays a dominant role not only in determining the geometrical size of the heliosphere, but also in the modulation of magnetic-field-induced asymmetries. More specifically, charge exchange between SW and CHISM protons and primary neutrals of interstellar origin always acts to decrease the asymmetry of the termination shock and the heliopause, which can otherwise be very large. This is particularly pronounced because the ionization ratio of the CHISM plasma is rather low. To investigate the deflection of the CHISM neutral hydrogen flow in the inner heliosphere from its original orientation in the unperturbed CHISM, we create two-dimensional neutral H velocity distributions in the inner heliosphere within a 45-degree circular conical surface with the apex at the Sun and the axis parallel to the interstellar flow vector. It is shown that the distribution of deflections is very anisotropic, that is, the most probable orientation of the H-atom velocity differs from its average direction. We show that the average deflection of the H-atom flow, for reasonable ISMF strengths, occurs mostly in the plane formed by the ISMF and CHISM velocity vectors at infinity. The possibility that the ISMF orientation may

This work is supported by NASA grants NNG05GD45G, NNG06GD48G, NNG06GD43G, and NNX08AJ21G, and NSF award ATM-0296114. Supercomputer time allocations are provided by DOE's INCITE project PSS001 and NCSA project MCA07S033.

N.V. Pogorelov (✉) · J. Heerikhuisen · G.P. Zank · S.N. Borovikov
Institute of Geophysics and Planetary Physics, University of California, Riverside, CA 92521, USA
e-mail: nikolaip@ucr.edu

J. Heerikhuisen
e-mail: jacobh@ucr.edu

G.P. Zank
e-mail: zank@ucr.edu

S.N. Borovikov
e-mail: sergeyb@ucr.edu

influence the 2–3 kHz radio emission, which is believed to originate in the outer heliosheath, is discussed.

Keywords ISM: kinematics and dynamics · Solar wind

1 Introduction

It has been known for about two decades (Fahr et al. 1988; Pogorelov and Matsuda 1998; Ratkiewicz et al. 1998) that the interstellar magnetic field (ISMF) of strength $\mathbf{B}_\infty$, by exerting pressure on the surface of the heliopause (HP), affects its shape and position with respect to the Sun and the direction of the CHISM plasma velocity vector $\mathbf{V}_\infty$. The asymmetry in the HP position is immediately seen in the shape of the heliospheric termination shock (TS). Following Linde et al. (1998) who considered a number of cases with $\mathbf{B}_\infty$ either parallel or perpendicular to $\mathbf{V}_\infty$, Pogorelov et al. (2004) revisited the problem of the ISMF influence of the heliospheric interface by analyzing the ISMF coupling with the interplanetary magnetic field (IMF) at the heliopause in an ideal MHD formulation. A range of different orientations of $\mathbf{B}_\infty$ with respect to $\mathbf{V}_\infty$ and the ecliptic plane was considered, and for all of them the changes in the HP and TS shape and orientations were analyzed. These studies remained rather academic until Lallement et al. (2005) suggested that the asymmetry in the plasma distribution on the interstellar side of the heliopause is responsible for the difference between the H-atom and the He-atom flow directions observed in the inner heliosphere in the *SOHO* SWAN experiment. This idea was confirmed by the calculations of Izmodenov et al. (2005), who estimated the direction of the H-atom flow in the inner heliosphere by analyzing statistically averaged trajectories on neutral hydrogen atoms. This was done in the absence of the IMF for a spherically-symmetric SW, which made the heliosphere symmetric with respect to the plane formed by $\mathbf{B}_\infty$ and $\mathbf{V}_\infty$ (a BV-plane). This means that the average neutral trajectory which starts at the CHISM point belonging to the BV-plane will remain in this plane. Meanwhile, trajectories that start at two points lying symmetrically with respect to the BV-plane will acquire out-of-plane velocity components oriented in opposite directions. Thus, the average out-of-plane deflection will be zero. Opher et al. (2006), remaining in the framework of the ideal MHD model, made the first attempt to quantify the TS asymmetries in the directions of the *Voyager 1* (*V1*) and *Voyager 2* (*V2*) spacecraft. However, in the absence of neutral H this model tends to exaggerate the effect of the ISMF on the heliospheric asymmetries considerably. Pogorelov et al. (2006) and Pogorelov and Zank (2006) also noticed that the flow of neutral hydrogen never preserves its original orientation in the unperturbed CHISM, even for $\mathbf{V}_\infty \parallel \mathbf{B}_\infty$. Moreover, in the presence of the IMF the deflection inevitably takes place both within and perpendicular to the BV-plane. This means that the hydrogen deflection plane (HDP) and the BV-plane generically do not coincide. The deflections parallel to the BV-plane and perpendicular to it become comparable if the angle between $\mathbf{B}_\infty$ and $\mathbf{V}_\infty$ is not small (Pogorelov and Zank 2006). To acquire a $4^\circ \pm 1^\circ$ hydrogen deflection observed in the *SOHO* SWAN experiment, one would need to assume a strong ISMF (perhaps greater than 4 μG). Magnetic fields of such strength should not be summarily disregarded because of the presumption that the TS/HP heliocentric distances may be too small for such fields. Since the magnetic pressure acts perpendicularly to magnetic field lines, plasma can actually move unobstructed along the lines. As a result, for $\mathbf{B}_\infty$ directed at small angles with respect to $\mathbf{V}_\infty$, the increase in $\mathbf{B}_\infty$ results in higher TS and HP stand-off distances in the upstream CHISM directions (Baranov and Krasnobaev 1971; Florinski et al. 2004). On the other hand, the presence of CHISM neutrals allows for 2D

(Florinski et al. 2004) and 3D (Pogorelov et al. 2006) solutions with the HP at finite distances from the Sun for sub-Alfvénic CHISM flows. These are impossible in the absence of neutrals. We note here that one of the theories of the origin of the Local Bubble (Cox and Helenius 2003) suggests a strong ISMF nearly parallel to the CHISM velocity vector. Since a multi-fluid analysis of the H flow deflection performed by Pogorelov and Zank (2006) and Pogorelov et al. (2007) assumes the fluid approximation for primary (born in the unperturbed CHISM) and secondary (born in the thermodynamically distinct SW and CHISM regions), one would want to see a kinetic analysis of neutral H trajectories. This is the main subject of the current paper. Additionally, we perform a comparison of numerical results obtained with the five-fluid (one plasma and four neutral fluids) and MHD-kinetic approaches. As suggested by Gurnett et al. (2006) and shown by Pogorelov et al. (2007), who followed the idea of Mitchell et al. (2008), the assumption of the BV-plane being parallel to the observed HDP results in band-like distributions of the ISMF strength in the outer heliosheath. Such bands are elongated nearly perpendicular to the BV-plane. Another approach, based on topological considerations to analyze the distribution of radio emission sources, was used by Opher et al. (2007). We explore this effect using our newly developed MHD-kinetic model (Heerikhuisen et al. 2006, 2007; Pogorelov et al. 2008a).

2 Heliospheric Asymmetry Induced by the ISMF

We performed numerical calculations in a Cartesian coordinate system (grid resolution is about 1.5 AU near the TS and 2.5 AU near the HP) with the origin at the Sun (Fig. 1). The x-axis is oriented along the Sun's rotation axis, which we assume to be perpendicular to the ecliptic plane (yz-plane). The z-axis belongs to the plane defined by the x-axis and $\mathbf{V}_\infty$, and is directed upstream into the CHISM. The y-axis completes the right coordinate system. The direction of the CHISM velocity is known (Moebius et al. 2004; Witte 2004) to be aligned with the vector $\mathbf{l}_{\rm He} = (-0.087156, 0, -0.9962)$. The HDP is defined by $\mathbf{l}_{\rm He}$ and the vector $\mathbf{l}_{\rm H}$ with the coordinates $(-0.1511, -0.04049, -0.9877)$ at

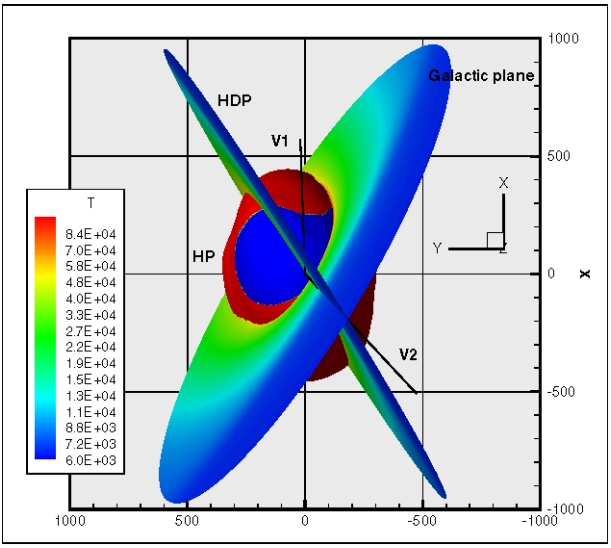

Fig. 1 Frontal view of the HP, HDP, Galactic plane, and *Voyager 1* and *2* trajectories. *Blue* and *red* colors on the surface of the HP correspond to the regions of negative and positive values of the ISMF radial component B_R, respectively. The planes have colors corresponding to the plasma temperature distributions in them. The HP is clearly asymmetric with respect to the BV-plane

which CHISM neutrals enter the inner heliosheath, according to the observations of Lallement et al. (2005). Throughout this paper we assume that $\mathbf{B}_\infty$ is aligned with the vector $\mathbf{l}_B = (-0.5, -0.2678, -0.82356)$. Thus, $\mathbf{B}_\infty$ belongs to the observed HDP and is directed into the southern hemisphere at an angle of 30° to the ecliptic plane. This means that the ISMF enters the heliosphere at the following ecliptic longitude and latitude: $\lambda \approx 238.8°$, $\beta \approx 22.9°$. This direction gave one of the largest *V1–V2* asymmetries of the TS in the two-fluid (one ion fluid and one neutral fluid) calculations of Pogorelov et al. (2007). Pogorelov et al. (2004) considered a case with $\mathbf{B}_\infty$ belonging to the plane tilted at 60° to the ecliptic plane, which was unwittingly identified with the Galactic plane, but in fact is very close to the observed HDP. As noticed by Stone et al. (2005), Opher et al. (2006), this orientation introduces east-west asymmetry of the TS which is consistent with the direction of energetic proton fluxes observed by *V1* and *V2*.

Voyager 2 observations (Stone et al. 2005) in the supersonic SW indicated that *V2* started measuring energetic charged particles at about 10 AU closer to the Sun than *V1*. This was demonstrably confirmed by the actual crossing of the TS by *V2* at ∼84 AU compared to ∼94 AU for *V1* (Stone et al. 2008). As can be seen from the model of Pogorelov et al. (2004), the ISMF with $\mathbf{B}_\infty$ at an angle of about 45° to $\mathbf{V}_\infty$ can indeed introduce a *V1–V2* asymmetry of this magnitude in the TS heliocentric distances. The figure showing this effect was adapted from Pogorelov et al. (2004) for the 2005 *Voyager* Senior Review Proposal. However, Pogorelov (2006) and Pogorelov et al. (2007) showed that this is an artifact of neglecting charge exchange between charged and neutral particles. Furthermore, the presence of neutrals does not allow *V2* to be directly connected by magnetic field lines to the TS at distances greater than 3 AU even for B_∞ as large as 3 μG (Pogorelov et al. 2007), while the corresponding fluxes of energetic protons were measured for at least two years (Stone et al. 2008). This implies a possible importance of time-dependent processes.

This is in distinction from the results of the ideal MHD models of Pogorelov et al. (2004) and Opher et al. (2006). The latter model, to arrive at some quantitative results, uniformly scales the ideal MHD solution to the known distance of the TS crossing by *V1*. The importance of this can be seen from the fact that the TS heliocentric distances can be 1.5 times larger if neutral particles are neglected and the scaling is nonuniform (Baranov and Malama 1993; Pauls et al. 1995; Zank et al. 1996; Zank 1999; Müller et al. 2008).

Here we assume that the CHISM plasma velocity, temperature and density are $V_\infty = 26.4\ \mathrm{km\,s^{-1}}$, $T_\infty = 6527\ \mathrm{K}$, and $n_\infty = 0.06\ \mathrm{cm^{-3}}$, respectively. It is assumed that the SW is spherically symmetric with the following parameters at 1 AU: $V_\mathrm{E} = 450\ \mathrm{km\,s^{-1}}$, $T_\mathrm{E} = 51\,100\ \mathrm{K}$, and $n_\mathrm{E} = 7.4\ \mathrm{cm^{-3}}$. The density of neutral hydrogen is $n_{\mathrm{H}\infty} = 0.15\ \mathrm{cm^{-3}}$. The magnitude of the ISMF vector is $\mathbf{B}_\infty = 3$ μG. The radial component of the IMF at 1 AU is set to 37.5 μG. Figure 1 shows the front view of the HP, obtained with our MHD-kinetic model, cut by the HDP as determined by Lallement et al. (2005), as well as the *V1* and *V2* trajectories. We also show the orientation of the Galactic plane. Figure 2 shows the distribution of the proton number density in the *V1–V2* plane. It is seen that, in agreement with the two-fluid calculations of Pogorelov et al. (2007), the asymmetry of the TS is minor. Figure 3 shows the distributions of the proton temperature in the directions of *V1* (solid black lines) and *V2* (solid red lines). For the sake of comparison, we also use dashed lines to show the same distributions obtained with a five-fluid model. The latter is based on the solution of ideal MHD equations to model the flow of protons and four coupled sets of Euler equations to simulate the flow of separate neutral H fluids. These consist of the parent CHISM neutrals (population 0) and those born in the outer heliosheath (population 1), inner heliosheath (population 2), and supersonic SW (population 3). It is interesting to see that if

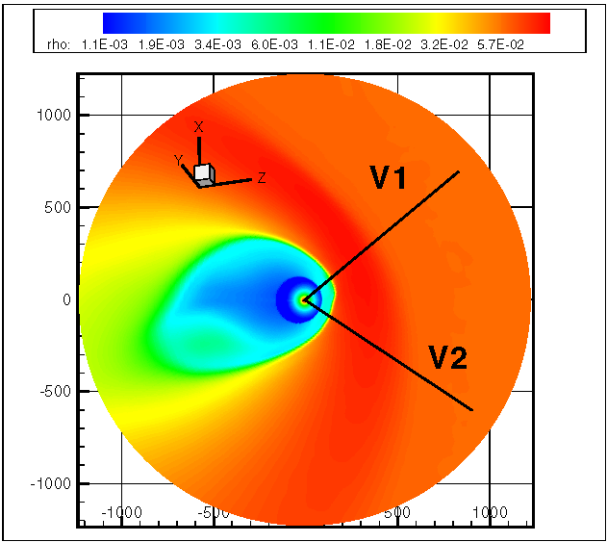

Fig. 2 Plasma number density distribution in the *V1*–*V2* plane. The *straight lines* show the *V1* and *V2* trajectories

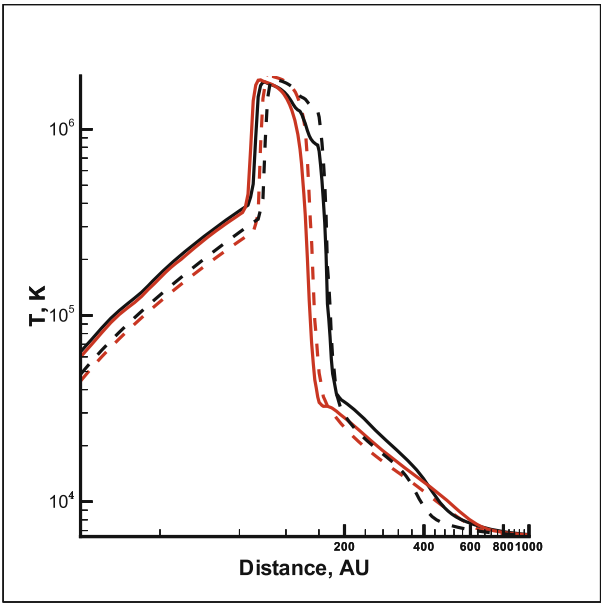

Fig. 3 The distributions of plasma temperature in the *V1* (*black lines*) and *V2* (*red lines*) directions. The results shown with *solid* and *dashed lines* are obtained with MHD-kinetic and five-fluid models, respectively (Pogorelov et al. 2008a)

charge exchange is treated kinetically, the bow shock, intrinsic to an equivalent ideal MHD model, disappears. This is because hot secondary neutral atoms created in the inner and outer heliosheaths have the ability to propagate upstream into the distant CHISM, where they heat the plasma ahead of the bow shock. One can notice that the introduction of population 1 neutrals considerably improves the solution in the outer heliosheath. On the other hand, the difference in the effective SW plasma temperature (the combination of the core and pick-up ion distributions) remains substantial because the filtration of neutral H into the HP is greater in the multi-fluid model than in the MHD-kinetic model.

There is a simple qualitative explanation of the symmetrizing effect of charge exchange. For the chosen SW and CHISM parameters, the neglect of neutral particles results in the HP rotating considerably, under the action of magnetic pressure, so that its nose is shifted to the south while the tail is shifted to the north with the appropriate shift of the nose westward (Pogorelov et al. 2007). As a result, the stagnation point of the CHISM plasma on the HP moves above the ecliptic plane. This creates an asymmetric distribution of the CHISM plasma in the outer heliosheath, which results in an enhanced charge exchange in this region. CHISM protons, decelerated and diverted at the HP, by exchanging their charge with CHISM neutrals, which are unimpeded by the HP, produce secondary (pick-up) ions with a pressure corresponding to the dynamic pressure of the parent atoms. These PUI's, in the process of their deceleration at the HP, exert additional pressure which acts to decrease the asymmetry of the HP by counterbalancing the ISMF pressure effect. A similar scenario works on the SW side of the HP. As seen from Fig. 3, the TS is closer to the Sun in the *V2* direction than in the *V1* direction by only about 3 AU in our MHD-kinetic simulation. In any event, the steady-state asymmetry is too small to ensure a *V2* crossing of the TS at a distance to the Sun closer by 10 AU than *V1*. Instead, it is likely that temporal variations in the SW ram pressure modify the TS location significantly (Scherer and Fahr 2003; Zank and Müller 2003; Borrmann and Fichtner 2005; Pogorelov et al. 2007; Washimi et al. 2007), thus supplementing the ISMF-pressure effect.

The MHD-neutral analysis of Pogorelov et al. (2007) shows that the east-west asymmetry of the TS due to the action of the ISMF lying in the observed HDP is also insufficiently large to allow *V2* to be directly (by less than a full winding of the IMF spiral) connected to the TS at distances larger than about 3 AU ahead of the TS. This is 2 AU smaller than the corresponding distance previously found in ideal MHD calculations by Opher et al. (2006) for a smaller ISMF (1.8 μG vs. 3 μG in this paper). The difference between ideal MHD and MHD-neutral results would, of course, have been larger for the same ISMF magnitude. Pogorelov et al. (2007) showed that energetic protons with energies below 7 MeV cannot reach *V2* by being connected to the TS indirectly. It is possible, in principle, to increase the TS asymmetry to 8 AU by increasing B_∞ to the surprisingly large value of 4 μG (Pogorelov et al. 2008b). This may result, however, in the H flow deflection being greater than that observed in the *SOHO* SWAN experiment (see the deflection results below). That is, these two effects are mutually related. Moreover, for magnetic fields of this strength, the radio emission conditions (Cairns and Zank 2002) will be satisfied in every point beyond the HP.

In Fig. 4 we compare the distributions of plasma density and magnetic field magnitude obtained with our five-fluid and MHD-kinetic models. Black, red, blue, and purple lines correspond to the directions $\phi = 180°, \theta = 35°$, $\phi = 0, \theta = 0$, $\phi = 0, \theta = 90°$, and $\phi = 0$, $\theta = 180°$, respectively. As usual, the angles ϕ and θ are measured from the x-axis in the xy-plane and from the z-axis, respectively. It is evident that the results obtained with these two substantially different models are in a very good qualitative and reasonable quantitative agreement.

Figure 5 shows the distributions of the neutral hydrogen atom density along the z-axis. Blue, purple, green, and red lines correspond to populations 0, 1, 2, and 3, respectively. Solid and dashed curves show the results obtained with our MHD-kinetic and five-fluid models, respectively. One will notice a discrepancy in the distributions of population 1 at large z, which is the result of a certain arbitrariness in our subdivision of populations 0 and 1 caused by the absence of a clearly defined bow shock. As noticed by Pogorelov et al. (2008a), hot neutrals born in the inner heliosheath propagate upstream into the CHISM, decelerate and heat it, thus eliminating a bow shock for the set of parameters used in this calculation. However, this discrepancy is of minor importance, since upstream propagating population 1 atoms have very low number density. It is notable that the results show

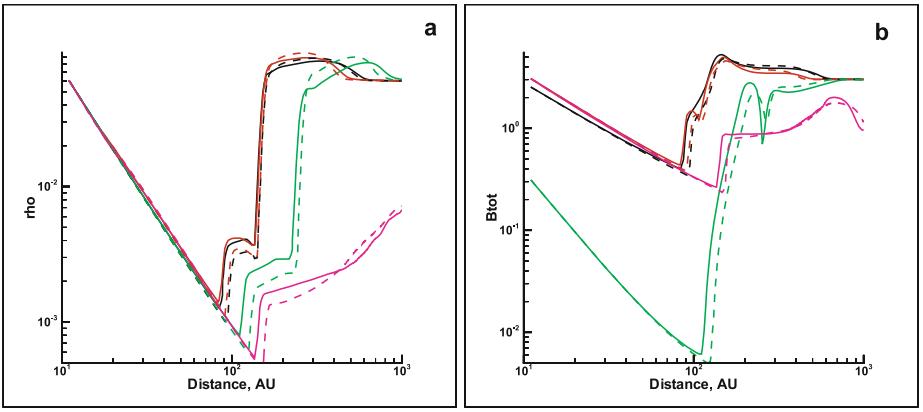

Fig. 4 The distributions of (**a**) plasma number density (in cm $^{-3}$) and (**b**) magnetic field magnitude (in μG) along the rays $\phi = 180°, \theta = 35°$ (*black lines*), $\phi = 0, \theta = 0$ (*red lines*), $\phi = 0, \theta = 90°$ (*green lines*), and $\phi = 0, \theta = 180°$ (*purple lines*). The results shown with *solid* and *dashed lines* are obtained with MHD-kinetic and five-fluid models, respectively

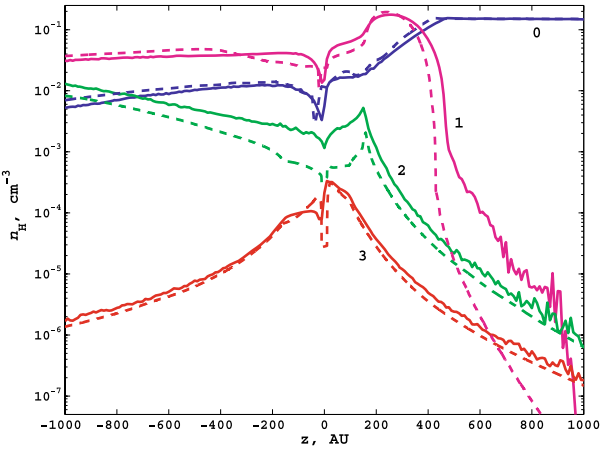

Fig. 5 The distributions of different populations of neutral hydrogen atoms along the z-axis. Blue, purple, green, and red lines correspond to populations 0, 1, 2, and 3, respectively. The results shown with solid and dashed lines are obtained with MHD-kinetic and five-fluid models, respectively

a very good qualitative agreement. As expected (see Heerikhuisen et al. 2006), the largest quantitative disagreement is in the distribution of population 2 neutrals. This is an intrinsic drawback of multi-fluid models which assume a Maxwellian distribution for these neutrals. This quantitative disparity can partially be leveled by the uncertainty in our knowledge of such properties of the CHISM as its ionization ratio and ion density.

To quantify the effect of the neutral H flow deflection, we run our kinetic neutral-atom code and collect statistics on the H-atom velocity distribution in the SW. We record the deflection from $\mathbf{V}_\infty$ of all H-atoms within a 45-degree cone about $\mathbf{V}_\infty$ out to 80 AU, both in the BV-plane and perpendicular to it, thus creating a two dimensional distribution of deflections. In Fig. 6 we show these for primary (population 0) CHISM H-atoms (top panel), secondary (population 1) H-atoms (middle panel), and the total (weighted) distribution (bottom panel) in the plane perpendicular to $\mathbf{V}_\infty$. Although the primary CHISM distribution starts out as Maxwellian, its interaction with the heliosphere results in a distribution of deflections that is obviously not isotropic. This is because charge-exchange losses may preferentially

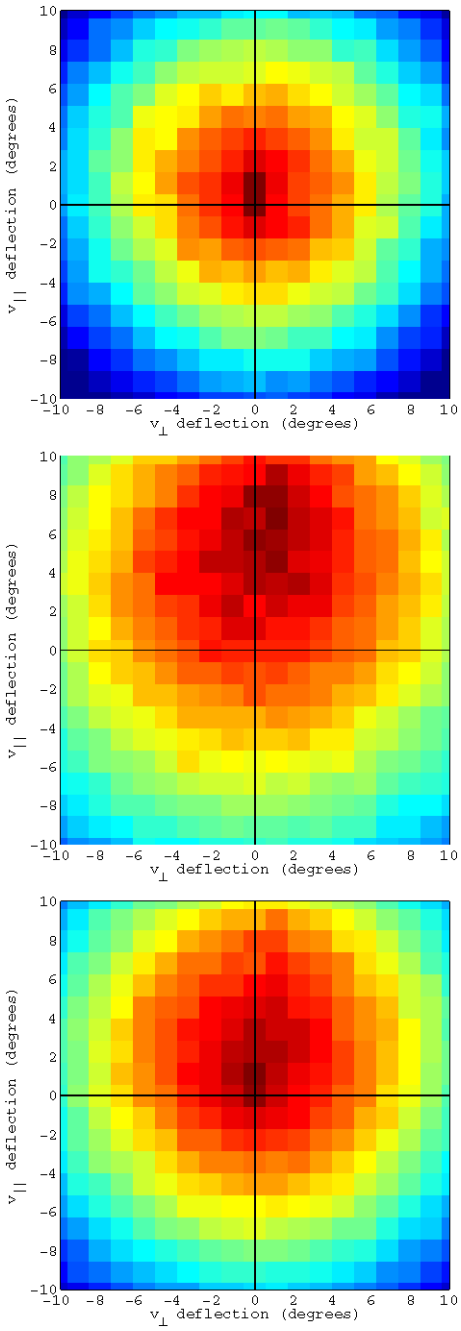

Fig. 6 Two-dimensional distribution of H-atom deflections from $\mathbf{V}_\infty$ in the plane perpendicular to the CHISM BV-plane (the interstellar perspective). *Top* are primary interstellar H-atoms, middle are secondary (i.e. last charge-exchange occurred in the outer heliosheath), while on the *bottom* is the combined distribution. The normal is determined by the vector product $\mathbf{l}_\mathrm{H} \times \mathbf{l}_\mathrm{He}$. The *darkest red* color corresponds to a particle count twice larger than that of the *darkest blue* color. (Pogorelov et al. 2008a)

cull a particular part of the distribution, due to asymmetric plasma flow and the dependence of the charge-exchange rate on the relative plasma flow speed. Secondary H-atoms (and the combined distribution, by extension) are clearly not isotropic, and the mean of the distribution does not coincide with its center, making it more difficult to quantify the overall

deflection. We find that the average deflection of primary neutrals is about 1.8° in the BV-plane and $-0.18°$ perpendicular to this plane. For secondary neutrals, the corresponding values are 4.7° and 0.15°, while for the combined population these are 3.8° and 0.05°. We point out, however, that the peaks of the distributions are not at these locations. Instead, the primary population shows a peak close to zero deflection and the most common deflection of the secondary neutrals is around 7° in the BV-plane and 1° out of it. It appears in this particular example, that the average deflection takes place almost entirely in the BV-plane. Thus, the actual angle between the BV-plane and the HDP is determined by the accuracy of measuring the H-flow direction in the *SOHO* SWAN experiment. Although we assume that the BV-plane is parallel to the average HDP, an additional deflection of the order of $\pm 1°$ perpendicular to the average HDP cannot be excluded. This gives us an estimate for the angle between the HDP and BV-plane at $\sim 15°$ (Pogorelov et al. 2007).

3 Sources of the 2–3 kHz radio emission

Radio emission in the 2–3 kHz range is thought to be generated when a global merged interaction region (GMIR) enters the outer heliosheath, where plasma is primed with an enhanced level of superthermal electrons (Cairns and Zank 2002). The origin of the hot electrons is due to their energization by lower-hybrid waves generated by pick-up ions, created from hot secondary neutrals born in the inner heliosheath as they propagate into the outer heliosheath and charge-exchange with the shocked plasma. These pick-up ions have a ring-beam distribution. Since ring-beam driven lower hybrid waves propagate almost perpendicularly to the magnetic field vector $\mathbf{B}$ in the outer heliosheath, Gurnett et al. (2006) suggested that regions which satisfy this property ahead of GMIRs might preferentially radiate in the 2–3 kHz range. If $\mathbf{B}_\infty$ lies in the observed HDP, the distribution of magnetic field strength in the outer heliosheath suggests that radio-emission-source distribution will be elongated in the direction almost perpendicular to it (Pogorelov et al. 2007). If one assumes, as was done for the purpose of identifying the distribution of radio emission sources by Opher et al. (2007), that a GMIR is spherical initially and preserves its sphericity after crossing the TS and the HP, then the regions on the HP and in the outer heliosheath where the radial component B_R of the magnetic field is equal to zero might be candidate regions for radio emission. The HP shown in Fig. 1 is painted with two colors, red and blue, which correspond to $B_R > 0$ and $B_R < 0$, respectively. The boundary between them is where $B_R = 0$. Here, like Pogorelov et al. (2007, 2008a), we see that there is a line that contains possible radio emission sources on the HP surface and is nearly perpendicular to the BV-plane. Note that *VI* detected radio emission sources distributed along the Galactic plane and also additional sources not aligned with the Galactic plane, called "ambiguous" by Kurth and Gurnett (2003). One can see, however, that the approach based on determining regions where $B_R = 0$ can exhibit the distributions of radio emission sources, which have many different orientation in space. From this viewpoint, the use of the space orientation of possible-radio-emission source distributions as a test bed (Opher et al. 2007) for the HDP definition is questionable. Of course, this is not necessary if we model the transport of neutral H atoms self-consistently with the plasma flow.

There is another issue that might be important if we suppose that the $B_R = 0$ condition can determine the distribution of radio emission sources. The line (or lines) defined by this equation on the surface of the HP is ambiguous because the exact location of the HP is not known with enough precision. It would be much more relevant to look at the shape of the surface $B_R = 0$ in the outer heliosheath. This is shown in Fig. 7, which is produced from

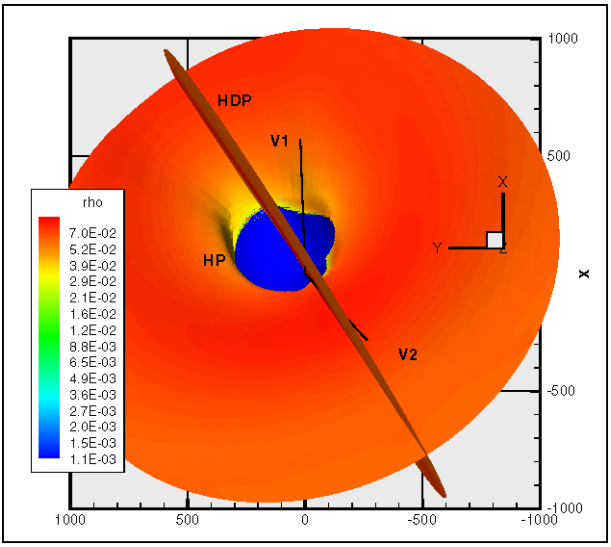

Fig. 7 The iso-surface $B_R = 0$ crossing the heliopause (compare with Fig. 1). The visible part of the HP surface has *blue* color indicating the region where $B_R < 0$. The *straight lines* corresponding to *V1* and *V2* trajectories and the HDP are also shown. 2–3 kHz radio emission sources are supposed to be distributed favorably on the $B_R = 0$ surface in the vicinity of the heliopause. This region is slightly elongated in the direction perpendicular to the HDP, although the lines of possible radio emission have no single particular orientation

Fig. 1 by adding the above-mentioned iso-surface and removing the Galactic plane. The blue color here shows negative values of B_R on the surface of the HP. The iso-surface $B_R = 0$ is colored according to the plasma density value on it. It is clear that the visible part of the boundary of the blue region and its vicinity belonging to the shown iso-surface are the best candidates for radio emission. It is seen that the domain is slightly elongated in the direction perpendicular to the HDP. On the iso-surface, there seems to exist a region containing the sources of possible radio emission, which is perpendicular to the HDP in the vicinity of the z-axis crossing the HP. There is also a region which is nearly parallel to the Galactic plane. However, there are also other regions that can be excluded only after analyzing whether physical conditions for radio emission are satisfied. It is therefore clear that one would need to use MHD-kinetic simulations to combine the condition $B_n = 0$, where B_n is the magnetic field component normal to a (nonspherical) GMIR shock surface, and utilize the physical conditions for generation of radio waves, if we are to use radio emission data as an additional constraint on the orientation of $\mathbf{B}_\infty$. As the angle between the HDP and the BV-plane can be as large as 15°, the ISMF orientation can presumably be adjusted to be consistent with the radio emission observations.

4 Conclusions

We have discussed the importance of charge exchange between charged and neutral particles for quantifying heliospheric asymmetries induced by the ISMF. It is clear, both from the qualitative analysis and the numerical modeling, that charge exchange tends to decrease the ISMF effect on the HP and, finally, on the TS. On the basis of a physical model that treats the motion of charged particles using ideal MHD equations and the transport of neutral particles kinetically, by solving the Boltzmann equation, we created distributions of neutral H velocity deflections from their original direction in the unperturbed CHISM, which is conventionally assumed to coincide with the neutral He velocity direction. We found that these distributions are highly anisotropic, with the most probable deflection not coinciding with the average deflection. It is however remarkable that, for the case considered in this

paper, the velocity deflection in the BV-plane is substantially larger than that in the direction perpendicular to the BV-plane. Since the deflection observed by Lallement et al. (2005) is $4° \pm 1°$, the meaning of the word "larger" is defined by the accuracy to which the deflection is measured. That is, any deflection of less than 1° in the direction perpendicular to the BV-plane is of no practical interest when comparing with the *SOHO* SWAN measurements. Being cautiously optimistic, we can conclude that, for reasonable ISMF strengths of less than 3 μG, the angle between the BV-plane and the observed HDP should not be larger than $\arctan(\tan 1°/\tan 4°) \approx 14°$ (see also Pogorelov et al. 2007, 2008a, 2008b). For $B_\infty = 3$ μG, the angle of 30° between $\mathbf{V}_\infty$ and $\mathbf{B}_\infty$ is sufficient to introduce a 4°-deflection of neutral H, which is consistent with the *SOHO* observations. For $B_\infty = 2.5$ μG, one might need to increase the angle to 45°. We showed that naive geometrical considerations do not allow us to determine the distribution of 2–3 kHz radio emission sources in the outer heliosheath. Moreover, ideal MHD simulations based on the models of Pogorelov et al. (2004), Opher et al. (2007) do not determine all geometrically-possible radio emission source distributions. To perform meaningful comparison of theoretical results with *Voyager* radio observations, one needs to combine numerical simulations of physical processes underlying the radio emission with the theoretical conditions ensuring its generation.

We performed a comparison of numerical results from different (MHD-kinetic and five-fluid) theoretical models of the heliospheric interface. The flow of charged particles is governed by the ideal MHD equations in both cases. The difference is in the way we treat the transport of neutral particles. The results for the distribution of protons obtained from our five-fluid and MHD-kinetic models are very consistent qualitatively. There are some quantitative differences, which are very well understood from a physical viewpoint, because kinetic transport of neutrals throughout the heliosphere differs from that based on the continuum description of multiple neutral fluids. Although the kinetic approach is physically relevant for the processes occurring in the outer heliosphere, one can easily see that the plasma distributions can be matched by modifying the CHISM properties to within the accuracy we know them. As far as the distribution of neutral particles is concerned, it is known (Heerikhuisen et al. 2006) that populations 0, 1, and 3 of neutrals are fairly well represented by Maxwellian distribution functions, while population 2 is not. As a result, the difference between our five-fluid and MHD-kinetic models is mostly due to the action of this population. While kinetic modeling of neutrals is unquestionably superior to a multi-fluid approach, the averaged results obtained with both approaches are very similar. The application of multi-fluid approaches might prove to be especially useful for realistic time-dependent problems addressing the propagation of SW transients through the heliosphere. Stochastic Monte Carlo approaches become very inefficient for problems where very small time (of the order of a day) and length (of the order of a fraction of AU) scales should be resolved. The question of physical validation of different SW–CHISM interaction models has been addressed recently by Müller et al. (2008).

Acknowledgements The authors are grateful to Horst Fichtner and Edward C. Stone for invaluable comments.

References

V.B. Baranov, K.V. Krasnobaev, Cosm. Res. **9**(4), 568–571 (1971)
V.B. Baranov, Y.G. Malama, J. Geophys. Res. **98**, 15157–15163 (1993)
T. Borrmann, H. Fichtner, Adv. Space Res. **35**, 2091–2101 (2005)
I.H. Cairns, G.P. Zank, Geophys. Res. Lett. **29**(7), 47-1–47-4 (2002)

D.P. Cox, L. Helenius, Astrophys. J. **583**, 205–228 (2003)
H.-J. Fahr, S. Grzedzielski, R. Ratkiewicz, Acta Geophys. **6**, 337–354 (1988)
V. Florinski, N.V. Pogorelov, G.P. Zank, B.E. Wood, D.P. Cox, Astrophys. J. **604**, 700–706 (2004)
D.A. Gurnett, W.S. Kurth, I.H. Cairns, J.J. Mitchell, in *Physics of the Inner Heliosheath: Voyager Observations, Theory, and Future Prospects*, ed. by J. Heerikhuisen et al. American Institute of Physics Conf. Proc., vol. 858 (AIP, New York, 2006), pp. 129–134
J. Heerikhuisen, V. Florinski, G.P. Zank, J. Geophys. Res. **111**, A06110 (2006)
J. Heerikhuisen, N.V. Pogorelov, G.P. Zank, V. Florinski, Astrophys. J. **655**, L53–L56 (2007)
V. Izmodenov, D. Alexashov, A. Myasnikov, Astron. Astrophys. **437**, L35–L38 (2005)
W.S. Kurth, D.A. Gurnett, J. Geophys. Res. **108**(A10), 8027 (2003)
R. Lallement, E. Quémerais, J.L. Bertaux, S. Ferron, D. Koutroumpa, R. Pellinen, Science **307**, 1447–1449 (2005)
T.J. Linde, T.I. Gombosi, P.L. Roe, K.G. Powell, D.L. DeZeeuw, J. Geophys. Res. **103**(A2), 1889–1904 (1998)
J.J. Mitchell, I.H. Cairns, N.V. Pogorelov, G.P. Zank, J. Geophys. Res. **113**(A4), A04102 (2008)
E. Moebius et al., Astron. Astrophys. **426**, 897–907 (2004)
H.-R. Müller, V. Florinski, J. Heerikhuisen, V.V. Izmodenov, K. Scherer, D. Alexashov, H.-J. Fahr, Astron. Astrophys. (2008, in press)
M. Opher, E.C. Stone, P.C. Liewer, Astrophys. J. **640**, L71–L74 (2006)
M. Opher, E.C. Stone, T.I. Gombosi, Science **316**, 875–878 (2007)
H.L. Pauls, G.P. Zank, L.L. Williams, J. Geophys. Res. **100**, 21595–21604 (1995)
N.V. Pogorelov, in *Physics of the Inner Heliosheath: Voyager Observations, Theory, and Future Prospects*, ed. by J. Heerikhuisen et al. American Institute of Physics Conf. Proc., vol. 858 (AIP, New York, 2006), pp. 3–13
N.V. Pogorelov, T. Matsuda, J. Geophys. Res. **103**(A1), 237–245 (1998)
N.V. Pogorelov, G.P. Zank, Astrophys. J. **636**, L161–L164 (2006)
N.V. Pogorelov, G.P. Zank, T. Ogino, Astrophys. J. **614**, 1007–1021 (2004)
N.V. Pogorelov, G.P. Zank, T. Ogino, Astrophys. J. **644**, 1299–1316 (2006)
N.V. Pogorelov, E.C. Stone, V. Florinski, G.P. Zank, Astrophys. J. **668**, 611–624 (2007)
N.V. Pogorelov, J. Heerikhuisen, G.P. Zank, Astrophys. J. **675**, L41–L44 (2008a)
N.V. Pogorelov, S.N. Borovikov, J. Heerikhuisen, I.A. Kryukov, G.P. Zank, in *Particle Acceleration and Transport in the Heliosphere and Beyond*, ed. by G. Li et al. American Institute of Physics Conf. Proc., vol. 1039 (AIP, New York, 2008b), pp. 410–417
R. Ratkiewicz, A. Barnes, G.A. Molvik, J.R. Spreiter, S.S. Stahara, M. Vinokur, Astron. Astrophys. **335**, 363–369 (1998)
K. Scherer, H.J. Fahr, Geophys. Res. Lett. **30**(2), 1045 (2003)
E.C. Stone, A.C. Cummings, F.B. McDonald, B. Heikkila, N. Lal, W.R. Webber, Science **309**, 2017–2020 (2005)
E.C. Stone, A.C. Cummings, F.B. McDonald, B. Heikkila, N. Lal, W.R. Webber, Nature **454**, 71–74 (2008)
H. Washimi, G.P. Zank, Q. Hu, T. Tanaka, K. Munakata, Astrophys. J. **670**, L139–L142 (2007)
M. Witte, Astron. Astrophys. **426**, 835–844 (2004)
G.P. Zank, Space Sci. Rev. **89**, 413–688 (1999)
G.P. Zank, H.-R. Müller, J. Geophys. Res. **108**(A6), 1240 (2003)
G.P. Zank, H.L. Pauls, L.L. Williams, D.T. Hall, J. Geophys. Res. **101**, 21639–21656 (1996)